


Article

Effects of SiO₂ Filler in the Shell and Wood Fiber in the Core on the Thermal Expansion of Core–Shell Wood/Polyethylene Composites

Lichao Sun ^{1,2,3} , Haiyang Zhou ^{1,3}, Guanggong Zong ⁴, Rongxian Ou ^{1,3}, Qi Fan ^{1,3}, Junjie Xu ^{1,3}, Xiaolong Hao ^{1,3,*} and Qiong Guo ^{1,3,*}

¹ Key Laboratory for Bio-based Materials and Energy of Ministry of Education, College of Materials and Energy, South China Agricultural University, 483 Wushan Road, Guangzhou 510642, China; sunlichao@scau.edu.cn (L.S.); zhouhaiyang@scau.edu.cn (H.Z.); rongxian_ou@scau.edu.cn (R.O.); fanqiscience@126.com (Q.F.); junjiexu@stu.scau.edu.cn (J.X.)

² Key Laboratory of Bio-based Material Science and Technology (Ministry of Education), Northeast Forestry University, Harbin 150040, China

³ Guangdong Laboratory of Lingnan Modern Agriculture, Guangzhou 510642, China

⁴ Art and Design Institute, Yangzhou University, 88 Daxue South Road, Yangzhou 225009, China; ggzong@yzu.edu.cn

* Correspondence: haoxiaolong@scau.edu.cn (X.H.); guoqiong@scau.edu.cn (Q.G.)

Received: 8 October 2020; Accepted: 22 October 2020; Published: 2 November 2020



Abstract: The influence of nano-silica (nSiO₂) and micro-silica (mSiO₂) in the shell and wood fiber filler in the core on the thermal expansion behavior of co-extruded wood/polyethylene composites (Co-WPCs) was investigated to optimize the thermal expansion resistance. The cut Co-WPCs samples showed anisotropic thermal expansion, and the thermal expansion strain and linear coefficient of thermal expansion (LCTE) decreased by filling the shell layer with rigid silica, especially nSiO₂. Finite element analysis indicated that the polymer-filled shell was mainly responsible for the thermal expansion. The entire Co-WPCs samples exhibited a lower thermal expansion strain than the cut Co-WPCs samples due to protection by the shell. Increasing the wood fiber content in the core significantly decreased the thermal expansion strain and LCTE of the Co-WPCs. The Co-WPCs whose core layer was filled with 70% wood fiber exhibited the greatest anisotropic thermal expansion.

Keywords: co-extrusion; wood plastic composites; thermal expansion; silica; core–shell structure

1. Introduction

Wood polymer composites (WPCs) usually consist of moisture-sensitive hydrophilic wood fibers and a temperature-sensitive hydrophobic polymer. The co-extrusion of these two components can prevent moisture absorption by coating a high polymer content in the shell layer [1,2]. In addition, co-extruded wood/polyethylene composites (Co-WPCs) with core–shell structures can also achieve better weatherability [3,4] and fire retardation [5,6] than regular WPCs [1,7]. However, Co-WPCs contain much more polymer in the shell layer, which may increase the thermal expansion more than regular WPCs [8]. Thermal expansion is an important component of dimensional stability, and excessive thermal expansion may restrict the use of Co-WPCs in outdoor applications.

Although some studies have reported that filling rigid materials in the shell layer can decrease the linear coefficient of thermal expansion (LCTE) of the entire Co-WPC, it also introduces some disadvantages, which are summarized in Table 1. The thermal expansion behavior of the Co-WPCs can be greatly affected by the filler loading and type in the shell layer [8]. Adding fibers or spherical particles into the polymer matrix can mechanically restrain polymer chains during heating or cooling

cycles, which can decrease the LCTE of composites [9]. The thermal expansion resistance has also been increased by improving the interfacial adhesion between the fillers and matrix [9,10].

Table 1. Summary of combinations of core–shell layer fillers and their effects on the thermal expansion of co-extruded wood/polyethylene composites (Co-WPCs).

Core Formulation	Shell Formulation	Variables	LCTE	Demerits	Refs
WF:HDPE:MAPE:Lubricant: = 50:40:4:6	HDPE/GF	Shell GF (0–40%)	↓	Only exceeded GF content (>30%) decreased LCTE	[11]
HDPE:WF:Lubricant:MAPE = 40:50:6:4	HDPE/WF/TPCC	Shell WF (0–25%), TPCC (6–18%)	↑	Only weak core lead to decreased LCTE	[8]
WF:HDPE:Talc:Lubricant:MAPE = 55:33:5:5:2	HDPE/BF	Shell BF (0–30%)	↑	LCTE of shell decreased, but increased LCTE of Co-WPCs	[9]
WF:HDPE:Talc:Lubricant:MAPE = 55:33:5:5:2	HDPE/Talc	Shell Talc (0–50%)	↑	LCTE of shell decreased, but increased LCTE of Co-WPCs	[10]
WF:HDPE:Talc:Lubricant:MAPE = 55:33:5:5:2	HDPE/BF/Talc	BF/Talc = 0/30, 10/20, 15/15, 20/10,30/0 wt % in shell	↑	LCTE of shell decreased slightly, but without LCTE of Co-WPCs	[12]

Note: WF = Wood fiber, HDPE = High-density polyethylene, MAPE = Maleic anhydride-grafted polyethylene, GF = Glass fiber, BF = Basalt fiber, TPCC = Treated precipitated calcium carbonate, LCTE = Linear coefficient of thermal expansion, ↑ = Increase, and ↓ = Decrease.

Low-cost micro- or nanoscale silica is the most common filler for improving the thermal stability and mechanical properties of polymers [13]. In our previous study, the flexural properties and creep resistance of Co-WPCs were improved by filling the shell layer with nano-silica [14]. In addition, the low LCTE of silica (0.5 ppm/°C) can also decrease the thermal expansion of the resulting composites when added at high concentrations into a polymer matrix (>100 ppm/°C) [13,15]. Therefore, using moderate amounts of silica in the shell may improve the thermal expansion resistance of Co-WPCs.

Similar to silica, the extremely low LCTE of wood fibers (10–30 ppm/°C) can drastically decrease the thermal expansion of polymers. The LCTE of WPCs decreased upon increasing the wood fiber loading [16–18]. Less filler in the shell layer, accompanied by high amounts of wood in the core layer, was used to form a high-performance, low-cost Co-WPC [19]. However, solid wood exhibited anisotropic thermal expansion due to the different LCTEs in the longitudinal, radial, and tangential directions [16]. Anisotropic thermal expansion was key to obtaining a tailored single-component LCTE without changing its chemical composition [20]. In addition, the wood fiber orientation in extruded WPCs led to anisotropic mechanical properties, which may have similar effects on the thermal expansion behavior. Thus, the influence of fiber orientation on anisotropic thermal expansion must be considered by filling the fibers with a high aspect ratio [15,21,22].

The objective of this article was to prepare Co-WPCs with silica in the shell layer and wood fiber in the core layer. To optimize the fabrication and thermal expansion resistance, the effects of silica amount in the shell layer and wood fiber in the core layer were investigated for their effects on the anisotropic thermal expansion of Co-WPCs systematically.

2. Materials and Methods

2.1. Materials

Wood fiber (*Populus adenopoda*, 40–80 mesh) was prepared using a special crusher. High-density polyethylene (HDPE) pellets (5000 s, 0.95 g cm^{-3}) were supplied by the Daqing Petrification Company (Daqing, China) with a melt flow rate of $0.90 \text{ g } 10 \text{ min}^{-1}$ according to ASTM 1238. Stearic acid was used as a lubricant and was supplied by Rizhisheng Company (Nantong, China) with a melting point of $65 \text{ }^\circ\text{C}$ and a density of 0.85 g cm^{-3} . Maleic anhydride-grafted polyethylene (MAPE) compatibilizer was supplied by Rizhisheng Company (Nantong, China) with a melt flow rate of $1.7 \text{ g } 10 \text{ min}^{-1}$. Two forms of silica were used: microscale silica (mSiO_2) with an average diameter of approximately $5 \text{ }\mu\text{m}$ (Xiang Lan Chemical Co., Ltd., Shanghai, China) and nanoscale silica (nSiO_2) with an average diameter of 15 nm (Shanghai Meng Tai Hu Industrial Co., Ltd., Shanghai, China) [14].

2.2. Preparation of the Composites

The wood fiber was dried in a drying oven for 24 h at $103 \pm 0.1 \text{ }^\circ\text{C}$ before being melt blended with HDPE, compatibilizer, and lubricant using a twin-screw extruder (L/D ratio of 30, SJSH-30, Nanjing Rubber Machinery Factory, Nanjing, China) to prepare WPC pellets for the core (Table 2). The temperatures ranged from 145 to $165 \text{ }^\circ\text{C}$. The nSiO_2 or mSiO_2 particles were initially melt blended with HDPE at the same temperature range using a twin-screw extruder in a specific ratio (Table 2). The resulting blends of HDPE, silica, and wood fiber were used as the shell layer using the same processing parameters. The shell layer granules were hot-pressed into a 4 mm layer at $180 \text{ }^\circ\text{C}$ with a pressure of 10 MPa for thermal expansion measurements.

The core and shell layer granules were extruded using co-extrusion equipment to prepare Co-WPCs, which the co-extrusion equipment including a single-screw extruder with L/D ratio of 45 (SJ-45, Nanjing Rubber Machinery Factory, Nanjing, China) and 30 (SJ-30, Nanjing SKY WIN Sci. & Tech. Dev. Co., Ltd., Nanjing, China), respectively. The resulting Co-WPCs were square, with sizes of $45 \times 6 \text{ mm}^2$ (length \times width) and a 1 mm shell thickness. The core layer without a shell layer ($45 \times 6 \text{ mm}^2$) was used as the control.

Table 2. Formulations of Co-WPCs filled with various contents of micro- or nanoscale silica and wood in the shell and core layers.

Sample ¹	Shell Layer (wt %)			Core Layer (wt %)			
	WF	HDPE	Silica	WF	HDPE	MAPE	Lubricant
Core	0	0	0	50	45	3	2
S0	10	90	0	50	45	3	2
S5	10	90	5	50	45	3	2
S10	10	90	10	50	45	3	2
S15	10	90	15	50	45	3	2
S20	10	90	20	50	45	3	2
W50	10	90	0	50	45	3	2
W60	10	90	0	60	35	3	2
W70	10	90	0	70	25	3	2

¹ W and S represent the wood fiber and silica, respectively, and the number behind W and S indicates the weight content.

2.3. Thermomechanical Analysis (TMA)

The thermal expansion of the cut Co-WPCs samples ($10 \times 10 \times 6 \text{ mm}^3$) was tested by a Q400 thermomechanical analyzer (TA Instruments Inc., New Castle, DE, USA). Before testing, all samples were heated at $60 \text{ }^\circ\text{C}$ for 24 h to eliminate the thermal history. Tests were run from -30 to $90 \text{ }^\circ\text{C}$ under

a high-purity nitrogen atmosphere with a 50 mL min^{-1} flow rate and a heating rate of $3 \text{ }^\circ\text{C min}^{-1}$. The thermal expansion along the thickness and extrusion direction (length) was measured (Figure 1).

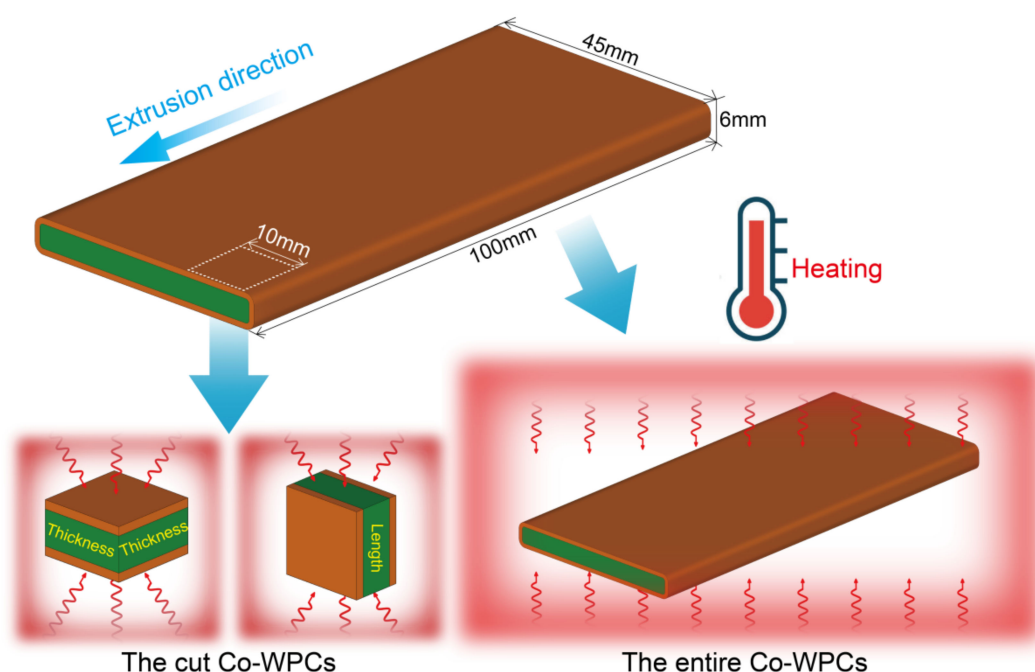


Figure 1. Schematic of the cut and entire Co-WPCs samples for thermal expansion tests.

The thermal expansion measured using TMA was unsuitable for the Co-WPCs samples due to their large sizes. The entire Co-WPC samples ($100 \times 45 \times 6 \text{ mm}^3$) were first measured at their original sizes at $25 \text{ }^\circ\text{C}$, and then their expanded sizes were recorded after being heated in an oven at $60 \text{ }^\circ\text{C}$ for 24 h to calculate the thermal expansion ratio. The thermal expansion of the entire Co-WPC samples along the thickness and extrusion direction (length) was measured (Figure 1).

2.4. Morphological Analysis

Thin sections with a thickness of 0.10–0.13 mm were cut from the Co-WPC profiles along and cross-planar transverse to the extrusion direction, respectively. The core–shell interface and wood fiber orientation were measured by a SMART-POL optical microscope (Chongqing Optec Instrument Co., Ltd., Chongqing, China).

2.5. Finite Element Analysis (FEA)

For simplicity, both the core and shell layers of the Co-WPCs were assumed to be isotropic. Abaqus 6.13 FEA software was used to numerically analyze the thermal expansion of the Co-WPCs samples using the parameters shown in Table 3. All sample dimensions used in the geometrical model were the same as those used during thermal expansion tests.

Table 3. The measured parameters of wood polymer composite (WPC) core and shell layers at $25 \text{ }^\circ\text{C}$ were used for finite element analysis [18,23].

Type	Young's Modulus (GPa)	Poisson Ratio	Density (g cm^{-3})	Average LCTE ($25 \rightarrow 60 \text{ }^\circ\text{C}$) ($10^{-6} \text{ }^\circ\text{C}^{-1}$)
Core Layer	2.0	0.30	1.2	$209^{\text{a}}/33^{\text{b}}$
S0 Shell Layer	0.71	0.38	0.95	234

^a and ^b represent the average LCTE of the core layer in thickness and extrusion direction, respectively.

3. Results

3.1. Subsection

The thermal expansion strain of the shell layer without filler (S0) was 29.74 ‰ at 90 °C and decreased to 18.96‰ for nSiO₂ (S20) and 8.84‰ for mSiO₂ (S20) (Figure 2a,b). This indicates that the thermal expansion resistance of the shell was greatly improved by adding nSiO₂, which has been shown to improve the mechanical properties by forming immobilization sites on HDPE chains via van der Waals forces [14,24,25]. These immobilization sites physically and mechanically restrained the HDPE matrix and improved the thermal resistance of the composites [13]. However, adding mSiO₂ only moderately and nonlinearly reduced the thermal expansion strain (Figure 2b), suggesting that mSiO₂ only had a small effect on the polymer matrix [26–28]. The reason can be explained by noting that the number of SiO₂ particles per unit volume increased 10⁹ times when changing from micro- to nanoscale SiO₂, which led to a significantly higher interfacial area between the SiO₂ and the polymer matrix [13].

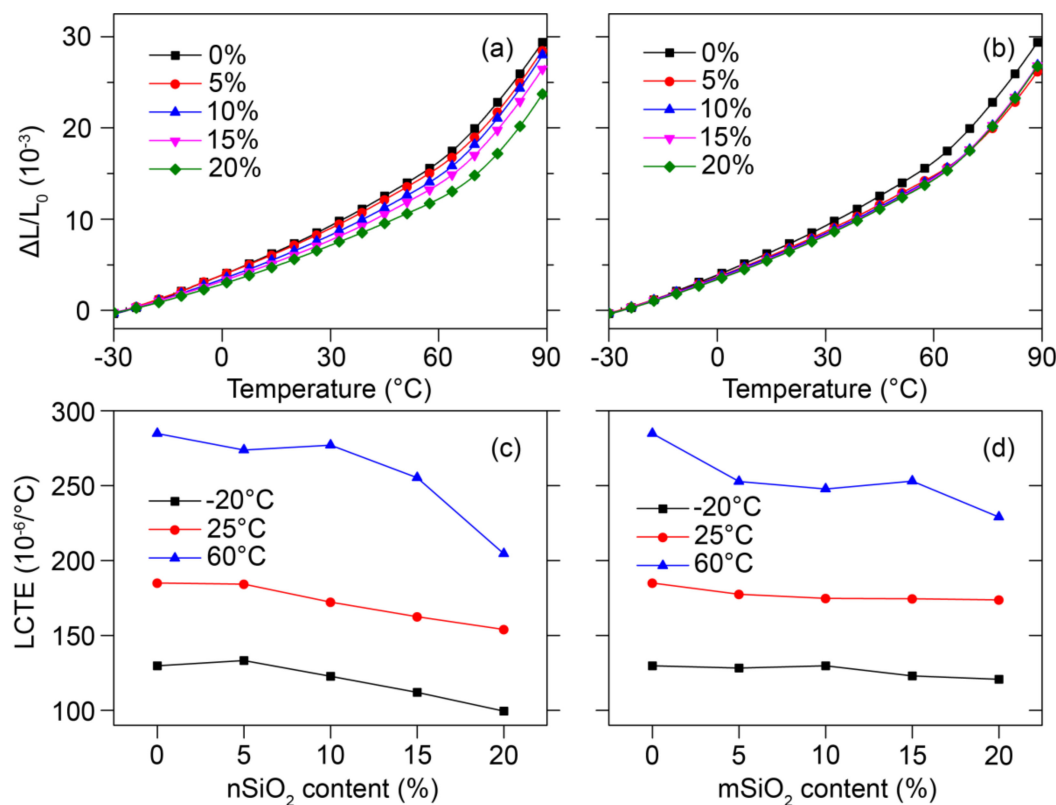


Figure 2. Thermal expansion strain of the shell layer samples: (a) nSiO₂ and (b) mSiO₂ fillers in shell layer, and LCTE as a function of silica content: (c) nSiO₂ and (d) mSiO₂ fillers in the shell layer.

The LCTE was obtained from the slope of the linear portion of the thermal expansion strain curve (Figure 2c,d). The LCTE of all samples increased upon increasing the temperature from −20 to 60 °C, illustrating the temperature sensitivity of the polymer LCTE. However, the LCTE significantly decreased upon increasing the nSiO₂ content, especially at 60 °C (≈60% decrease). Similar to the thermal expansion strain, the LCTE only moderately decreased after the addition of mSiO₂, indicating that the LCTE of the WPCs depended mainly upon the polymer matrix [17]. In addition, using low-LCTE rigid fillers may reduce the thermal expansion of the resulting polymer composites [9,13,15,29].

3.2. Thermal Expansion Anisotropy of Co-WPCs Silica Filler in the Shell Layer

The co-extruded sample (S0) exhibited a 16.41% higher thermal expansion strain at 90 °C than the pure core layer in the thickness direction (Figure 3a). This was attributed to the small amount of wood fiber in the shell layer, which had only a slight stiffness. Incorporating nSiO₂ in the shell considerably decreased the thermal expansion strain of Co-WPCs because of its smaller size effect, which was lower than the core layer, and S20 showed the largest decrease. Adding mSiO₂ in the shell only slightly decreased the thermal expansion strain compared with nSiO₂, but it was still higher than the pure core layer (Figure 3b). The lack of a positive effect of mSiO₂ on the LCTE can be viewed as the absence of nanoscale effects, which is consistent with the shell layer results. Since the enhanced mechanical properties of the shell contributed to those of the entire Co-WPC [7,8], these results illustrate that incorporating rigid SiO₂ in the shell layer can substantially improve the thermal expansion resistance of the Co-WPCs.

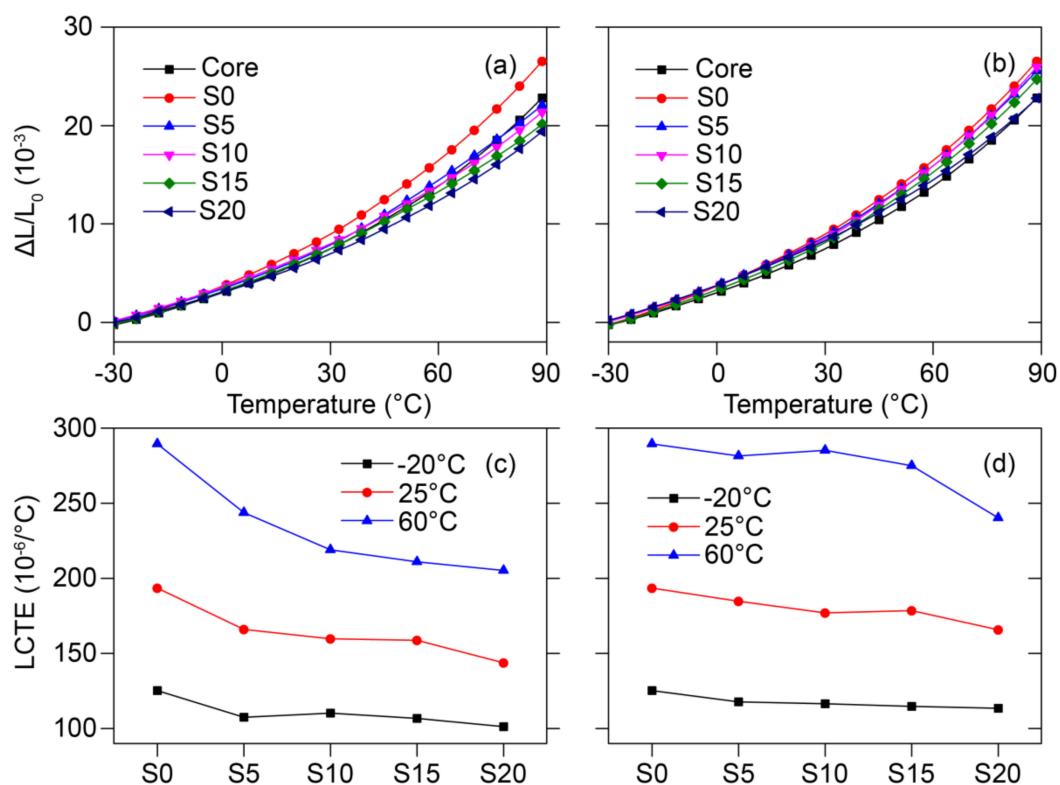


Figure 3. Thermal expansion strain of the cut Co-WPCs in the thickness direction: (a) nSiO₂ and (b) mSiO₂ fillers in shell layer, and LCTE as a function of silica content: (c) nSiO₂ and (d) mSiO₂ fillers in the shell layer.

The Co-WPCs exhibited much lower thermal expansion strain in the length (or extrusion) direction than along the thickness direction (Figure 4), which may be due to the orientation effect of wood fiber, especially in the core. On the sectioned surface of the Co-WPCs, wood fibers were oriented in the shell and core layers along the extrusion direction due to the high extrusion pressure (Figure 5a) [30,31]. In addition, the shell and core layers exhibited proper interfacial adhesion, since the same HDPE matrix was used to integrate the two layers into a coherent material at sufficient temperature and pressure. However, the wood fibers were randomly distributed in the cross-section transverse to the extrusion direction (Figure 5b), which lead to a higher thermal expansion strain in the thickness direction. In the extrusion direction, high-aspect-ratio wood fiber decreased the LCTE of the WPCs to mechanically restrain the polymer matrix from deforming by changing the thermal stress distribution inside the WPCs [13]. The high-aspect-ratio fillers restricted the polymer chain relaxation more than the spherical fillers [13]. In addition, the thermal expansion strains of Co-WPCs decreased remarkably

by filling the shell with nSiO₂ or mSiO₂ compared with S0; however, they were still higher than the core layer (Figure 4a,b). The LCTE values greatly decreased upon increasing the nSiO₂ content and exhibited comparable levels to the core layer in S10, even when heated from −20 to 60 °C (Figure 4c). When mSiO₂ was incorporated in the shell layer, the LCTE only slightly increased when the shell layer changed from S10 to S20 (Figure 4d). These results suggest that the thermal expansion was dominated by the oriented core layer, and the rigid SiO₂ filler in the shell produced a cooperative effect that decreased thermal expansion in the extrusion direction. However, the LCTE in the extrusion direction was lower in the thickness direction, which may lead to greater thermal expansion when the dimensions are much larger in the extrusion direction in practical applications.

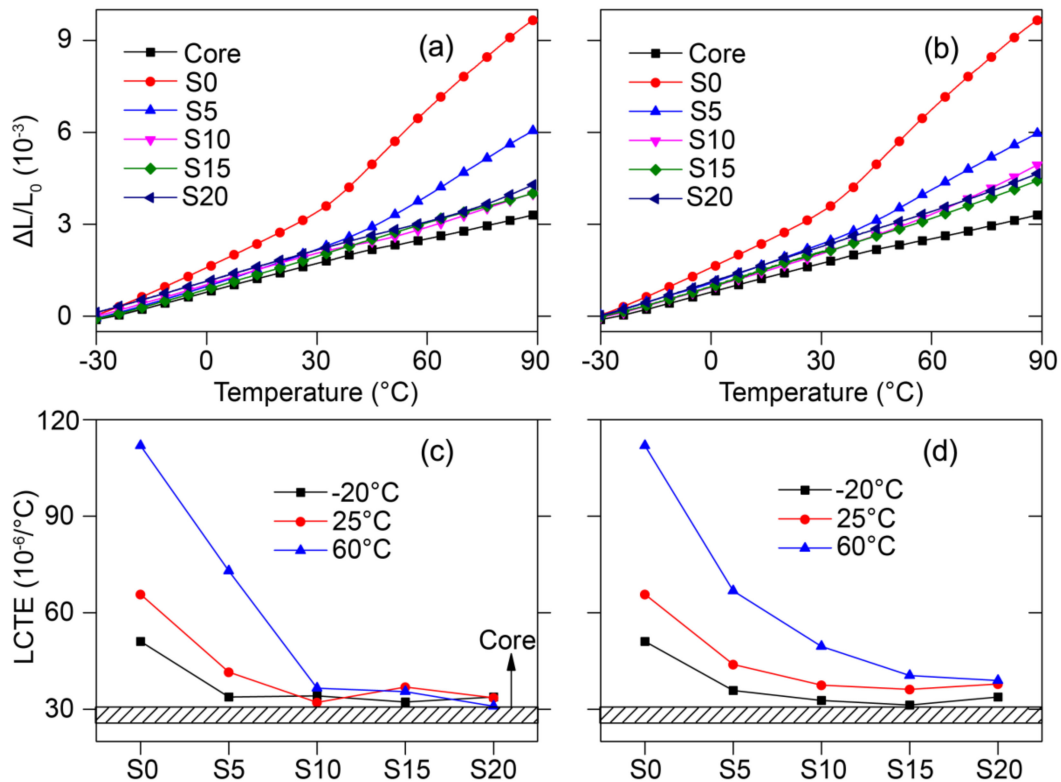


Figure 4. Thermal expansion strain of the cut Co-WPCs in the extrusion direction: (a) nSiO₂ and (b) mSiO₂ fillers in shell layer, and LCTE as a function of silica content: (c) nSiO₂ and (d) mSiO₂ fillers in the shell layer.

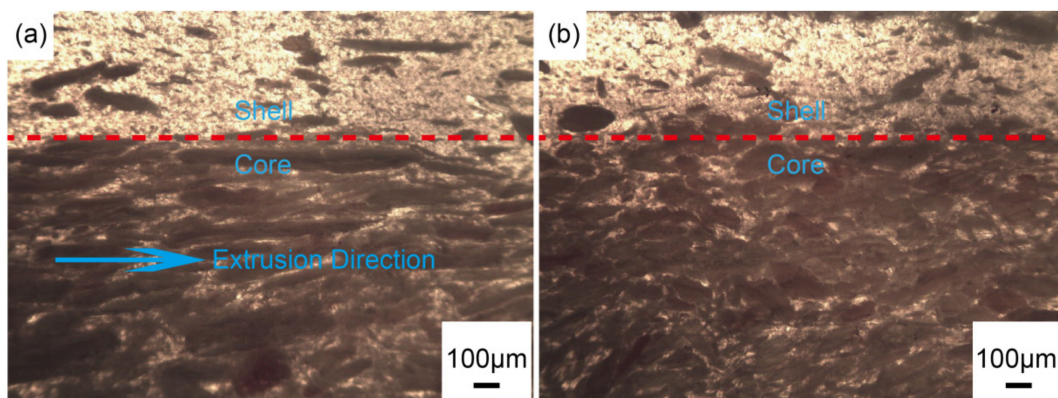


Figure 5. Optical micrographs of Co-WPCs (S0) along the extrusion direction ((a) $\times 40$) and in the cross-section transverse to the extrusion direction ((b) $\times 40$).

To analyze why anisotropic thermal expansion occurred in the Co-WPCs, the thermal expansion behavior was simulated by FEA from 25 to 60 °C in the thickness and extrusion directions (Figure 6). For brevity, the core and shell layers of Co-WPCs were assumed to be homogenous and only showed different LCTE values in the thickness (y-axis) and extrusion (z-axis) directions. Higher thermal expansion values were observed for Co-WPCs than the control, indicating poorer thermal expansion resistance. The shell layer was the main body that underwent thermal expansion in the extrusion direction due to its higher LCTE, showing that the wood fiber orientation determined the anisotropic expansion of the Co-WPCs.

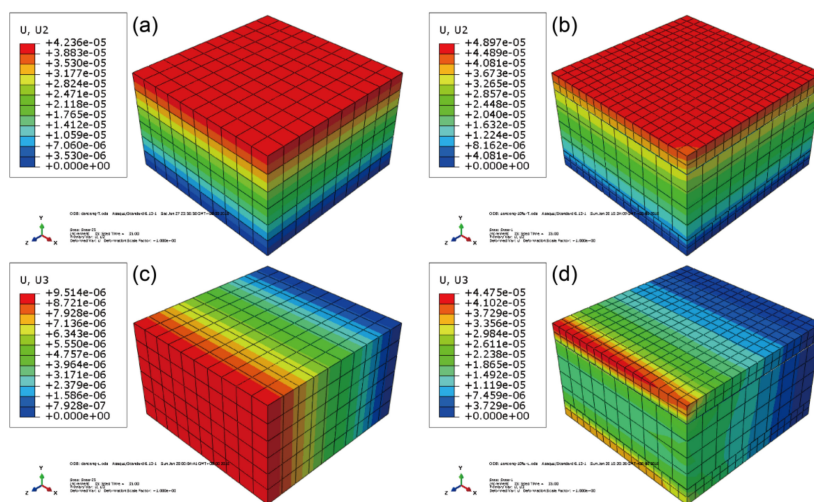


Figure 6. Simulated thermal expansion strain of the cut Co-WPCs in the thickness direction: (a) single core layer and (b) Co-WPCs (S0); in the extrusion directions: (c) single core layer and (d) Co-WPCs (S0).

The thermal expansion specimens used for TMA were cut from Co-WPCs, which cannot reflect the protective effect of the coating shell layer, and the thermal expansion behavior of the entire Co-WPCs samples (100 mm × 45 mm × 6 mm) was further analyzed. The thermal expansion strain showed the same magnitude as the above results but was much lower (Figure 7), indicating that the coating shell layer can mechanically restrict the entire Co-WPCs. After using rigid silica filler in the shell, the entire Co-WPCs (S10 and S20) showed smaller dimensional changes than the core layer (control) in the thickness and extrusion directions. The simulation results also demonstrated the protective effect of the coating shell layer on the thermal expansion resistance of the entire Co-WPCs (Figures S1 and S2).

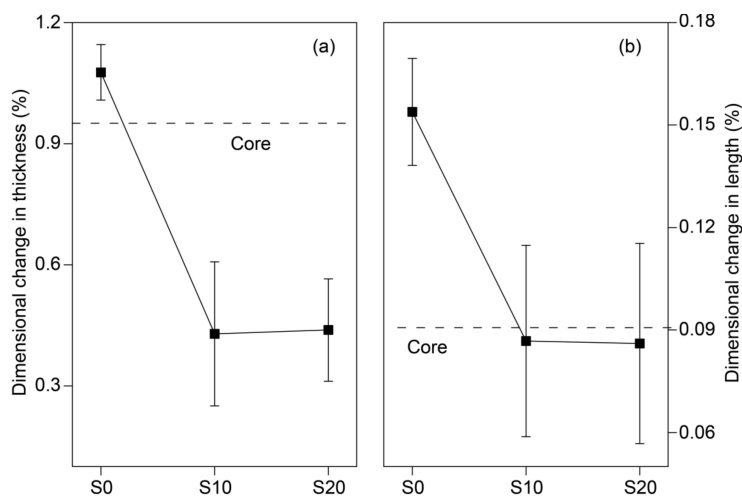


Figure 7. Thermal expansion strain of the entire Co-WPCs with nSiO₂ filler in the shell in the thickness (a) and length directions (b).

3.3. Thermal Expansion Anisotropy of Co-WPCs with High Filler Contents in the Core

Increasing the wood fiber from 10% to 30% linearly decreased the thermal expansion strain of the shell layer (Figure S3). The thermal expansion strain and LCTE of Co-WPCs were also moderately reduced by increasing the wood fiber in the shell layer but were still higher than those of the control (Figure S4), which demonstrates a lower efficiency than rigid silica. Upon increasing the amount of wood fiber in the shell layer, the entire Co-WPCs showed a smaller dimensional change in the thickness direction and comparable dimensional change in extrusion direction than the control (Figure S5).

Therefore, the effect of high wood fiber filler contents in the core layer on the anisotropic thermal expansion of Co-WPCs was analyzed (Figure 8). Increasing the wood fiber to 70% in the core layer distinctly decreased the thermal expansion strain of Co-WPCs in the thickness and extrusion directions (Figure 8a,b). The LCTE values also linearly decreased, especially at 60 °C (Figure 8c,d), which meant that the wood fiber ratio of the core primarily determined the thermal expansion of Co-WPCs. Core layers with high filler contents also exhibited greater anisotropic thermal expansion due to the lower LCTE in the extrusion direction.

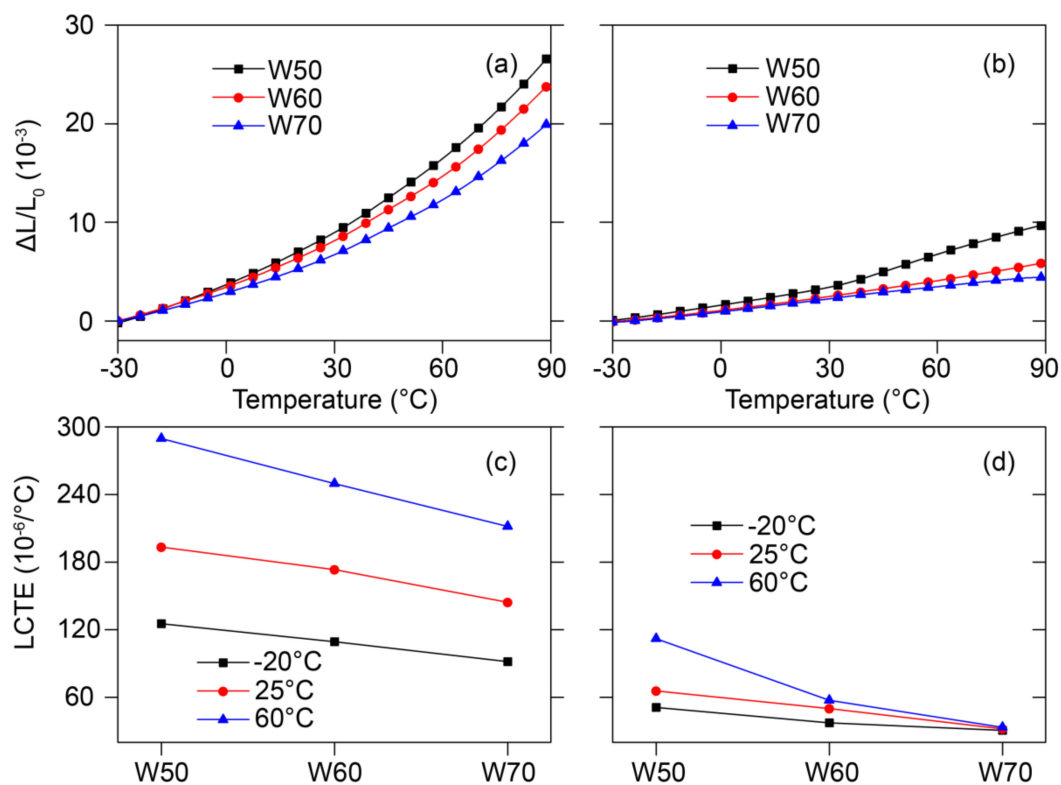


Figure 8. Thermal expansion strain as a function of temperature of Co-WPCs with high filler content: (a) in the thickness and (b) length directions, and LCTE in the thickness (c) and length directions (d).

4. Conclusions

The thermal expansion strain of cut Co-WPCs samples decreased upon increasing the silica content in the shell layer, especially for nSiO₂. The LCTE values of Co-WPCs also decreased upon increasing the silica content but showed anisotropic thermal expansion due to the wood fiber orientation in the core layer. Increasing the rigid silica content in the shell was an effective method to reduce the thermal expansion strain of the Co-WPCs. The entire Co-WPCs samples exhibited lower thermal expansion strain than the cut Co-WPCs samples, illustrating the protective effect of the coating shell layer. The high wood fiber filler content in the core decreased the thermal expansion strain and LCTE in the thickness and extrusion directions, respectively. Thus, the optimized formulation on both the shell and core layers is a suitable method for optimizing the thermal expansion resistance of Co-WPCs.

Supplementary Materials: The supplementary materials are available online at <http://www.mdpi.com/2073-4360/12/11/2570/s1>, Figure S1: Simulated thermal expansion strain values the entire Co-WPCs in the thickness direction: (a) single core layer (W50), (b) S0, (c) S10 and (d) S20, Figure S2: Simulated thermal expansion strain values of the entire Co-WPCs in the extrusion direction: (a) single core layer (W50), (b) S0, (c) S10 and (d) S20, Figure S3: Thermal expansion strain of the shell filling with different wood fiber contents, Figure S4: Thermal expansion strain of the cut Co-WPCs (W50) filling with different wood fiber in shell layer in the thickness (a) and extrusion directions (b); and LCTE in thickness direction (c) and extrusion directions (d), Figure S5: Thermal expansion strain of the entire Co-WPCs (W50) filling with different wood fiber in shell layer in the thickness (a) and extrusion directions (b).

Author Contributions: Conceptualization, L.S. and Q.G.; methodology, X.H.; software, H.Z.; validation, G.Z., R.O. and Q.F.; formal analysis, L.S.; data curation, J.X.; writing—original draft preparation, L.S.; writing—review and editing, X.H. and Q.G. All authors have read and agreed to the published version of the manuscript.

Funding: This research was funded by the National Natural Science Foundation of China (Grant Nos. 31700494, 31870547 and 31901251) and the Project funded by China Postdoctoral Science Foundation (Grant No. 2019M652919) to support this work. The authors also express thanks to the supported by Key Laboratory of Bio-based Material Science & Technology (Northeast Forestry University), Ministry of Education (Grant No. SWZ-ZD201905), the Project of Key Disciplines of Forestry Engineering of Bureau of Education of Guangzhou Municipality, the National Key Research and Development Program of China (Grant No. 2019YFD1101204), and the Project of Guangzhou Municipal Key Laboratory of Woody Biomass Functional New Materials (Grant No. 201905010005).

Conflicts of Interest: The authors declare no conflict of interest.

References

1. Yao, F.; Wu, Q. Coextruded polyethylene and wood-flour composite: Effect of shell thickness, wood loading, and core quality. *J. Appl. Polym. Sci.* **2010**, *118*, 3594–3601. [[CrossRef](#)]
2. Jin, S.; Matuana, L.M. Wood/plastic composites co-extruded with multi-walled carbon nanotube-filled rigid poly(vinyl chloride) cap layer. *Polym. Int.* **2010**, *59*, 648–657. [[CrossRef](#)]
3. Matuana, L.M.; Jin, S.; Stark, N.M. Ultraviolet weathering of HDPE/wood-flour composites coextruded with a clear HDPE cap layer. *Polym. Degrad. Stabil.* **2011**, *96*, 97–106. [[CrossRef](#)]
4. Jin, S.; Stark, N.M.; Matuana, L.M. Influence of a stabilized cap layer on the photodegradation of coextruded high density polyethylene/wood-flour composites. *J. Vinyl Addit. Technol.* **2013**, *19*, 239–249. [[CrossRef](#)]
5. Sun, L.; Wu, Q.; Xie, Y.; Wang, F.; Wang, Q. Thermal degradation and flammability properties of multilayer structured wood fiber and polypropylene composites with fire retardants. *RSC Adv.* **2016**, *6*, 13890–13897. [[CrossRef](#)]
6. Turku, I.; Nikolaeva, M.; Kärki, T. The effect of fire retardants on the flammability, mechanical properties, and wettability of co-extruded pp-based wood-plastic composites. *Bioresources* **2014**, *9*, 1539–1551. [[CrossRef](#)]
7. Jin, S.; Matuana, L.M. Coextruded PVC/wood-flour composites with WPC cap layers. *J. Vinyl Addit. Technol.* **2008**, *14*, 197–203. [[CrossRef](#)]
8. Kim, B.-J.; Yao, F.; Han, G.; Wang, Q.; Wu, Q. Mechanical and physical properties of core-shell structured wood plastic composites: Effect of shells with hybrid mineral and wood fillers. *Compos. Part B* **2013**, *45*, 1040–1048. [[CrossRef](#)]
9. Wu, Q.; Chi, K.; Wu, Y.; Lee, S. Mechanical, thermal expansion, and flammability properties of co-extruded wood polymer composites with basalt fiber reinforced shells. *Mater. Des.* **2014**, *60*, 334–342. [[CrossRef](#)]
10. Huang, R.; Kim, B.-J.; Lee, S.; Yang, Z.; Wu, Q. Co-extruded wood-plastic composites with talc-filled shells: Morphology, mechanical, and thermal expansion performance. *Bioresources* **2013**, *8*, 2283–2299. [[CrossRef](#)]
11. Huang, R.; Xiong, W.; Xu, X.; Wu, Q. Thermal expansion behaviour of coextruded WPC with glass fiber reinforced shells. *Bioresources* **2012**, *7*, 5514–5526. [[CrossRef](#)]
12. Huang, R.; Mei, C.; Xu, X.; Kärki, T.; Lee, S.; Wu, Q. Effect of hybrid talc-basalt fillers in the shell layer on thermal and mechanical performance of co-extruded wood plastic composites. *Materials* **2015**, *8*, 8510–8523. [[CrossRef](#)] [[PubMed](#)]
13. Ren, L.; Pashayi, K.; Fard, H.R.; Kotha, S.P.; Borca-Tasciuc, T.; Ozisik, R. Engineering the coefficient of thermal expansion and thermal conductivity of polymers filled with high aspect ratio silica nanofibers. *Compos. Part B* **2014**, *58*, 228–234. [[CrossRef](#)]
14. Hao, X.; Zhou, H.; Xie, Y.; Xiao, Z.; Wang, H.; Wang, Q. Mechanical reinforcement and creep resistance of coextruded wood flour/polyethylene composites by shell-layer treatment with nano- and micro-SiO₂ particles. *Polym. Compos.* **2018**, 1576–1584. [[CrossRef](#)]

15. Takenaka, K.; Ichigo, M. Thermal expansion adjustable polymer matrix composites with giant negative thermal expansion filler. *Compos. Sci. Technol.* **2014**, *104*, 47–51. [[CrossRef](#)]
16. Yang, H.S.; Wolcott, M.P.; Kim, H.-S.; Kim, H.-J. Thermal properties of lignocellulosic filler-thermoplastic polymer bio-composites. *J. Therm. Anal. Calorim.* **2005**, *82*, 157–160. [[CrossRef](#)]
17. Nakagaito, A.N.; Yano, H. The effect of fiber content on the mechanical and thermal expansion properties of biocomposites based on microfibrillated cellulose. *Cellulose* **2008**, *15*, 555–559. [[CrossRef](#)]
18. Hao, X.; Zhou, H.; Xie, Y.; Mu, H.; Wang, Q. Sandwich-structured wood flour/HDPE composite panels: Reinforcement using a linear low-density polyethylene core layer. *Constr. Build Mater.* **2018**, *164*, 489–496. [[CrossRef](#)]
19. Hao, X.; Yi, X.; Sun, L.; Tu, D.; Wang, Q.; Ou, R. Mechanical properties, creep resistance, and dimensional stability of core/shell structured wood flour/polyethylene composites with highly filled core layer. *Constr. Build Mater.* **2019**, *226*, 879–887. [[CrossRef](#)]
20. Monroe, J.A.; Gehring, D.; Karaman, I.; Arroyave, R.; Brown, D.W.; Clausen, B. Tailored thermal expansion alloys. *Acta Mater.* **2016**, *102*, 333–341. [[CrossRef](#)]
21. Baschek, G.; Hartwig, G. Parameters influencing the thermal expansion of polymers and fibre composites. *Cryogenics* **1998**, *38*, 99–103. [[CrossRef](#)]
22. Shirasu, K.; Nakamura, A.; Yamamoto, G.; Ogasawara, T.; Shimamura, Y.; Inoue, Y.; Hashida, T. Potential use of CNTs for production of zero thermal expansion coefficient composite materials: An experimental evaluation of axial thermal expansion coefficient of CNTs using a combination of thermal expansion and uniaxial tensile tests. *Compos. Part A* **2017**, *95*, 152–160. [[CrossRef](#)]
23. Cen-Puc, M.; Oliva-Avilés, A.I.; Avilés, F. Thermoresistive mechanisms of carbon nanotube/polymer composites. *Phys. E* **2018**, *95*, 41–50. [[CrossRef](#)]
24. Zhou, H.; Hao, X.; Wang, H.; Wang, X.; Liu, T.; Xie, Y.; Wang, Q. The reinforcement efficacy of nano- and microscale silica for extruded wood flour/HDPE composites: The effects of dispersion patterns and interfacial modification. *J. Mater. Sci.* **2018**, *53*, 1899–1910. [[CrossRef](#)]
25. Mammeri, F.; Bourhis, E.L.; Rozes, L.; Sanchez, C. Mechanical properties of hybrid organic–inorganic materials. *J. Mater. Chem.* **2005**, *15*, 3787. [[CrossRef](#)]
26. Wu, C.; Zhang, M.; Rong, M.; Friedrich, K. Silica nanoparticles filled polypropylene: Effects of particle surface treatment, matrix ductility and particle species on mechanical performance of the composites. *Compos. Sci. Technol.* **2005**, *65*, 635–645. [[CrossRef](#)]
27. Shariati, M.; Farzi, G.; Dadrasi, A. Mechanical properties and energy absorption capability of thin-walled square columns of silica/epoxy nanocomposite. *Constr. Build Mater.* **2015**, *78*, 362–368. [[CrossRef](#)]
28. Pourhossaini, M.-R.; Razzaghi-Kashani, M. Effect of silica particle size on chain dynamics and frictional properties of styrene butadiene rubber nano and micro composites. *Polymer* **2014**, *55*, 2279–2284. [[CrossRef](#)]
29. Takezawa, A.; Kobashi, M.; Takezawa, A.; Kobashi, M. Design methodology for porous composites with tunable thermal expansion produced by multi-material topology optimization and additive manufacturing. *Compos. Part B* **2018**, *131*, 21–29. [[CrossRef](#)]
30. Migneault, S.; Koubaa, A.; Erchiqui, F.; Chaala, A.; Englund, K.; Wolcott, M.P. Application of micromechanical models to tensile properties of wood–plastic composites. *Wood Sci. Technol.* **2010**, *45*, 521–532. [[CrossRef](#)]
31. Hao, X.; Zhou, H.; Mu, B.; Chen, L.; Guo, Q.; Yi, X.; Sun, L.; Wang, Q.; Ou, R. Effects of fiber geometry and orientation distribution on the anisotropy of mechanical properties, creep behavior, and thermal expansion of natural fiber/HDPE composites. *Compos. Part B* **2020**, *185*, 107778. [[CrossRef](#)]

Publisher’s Note: MDPI stays neutral with regard to jurisdictional claims in published maps and institutional affiliations.



© 2020 by the authors. Licensee MDPI, Basel, Switzerland. This article is an open access article distributed under the terms and conditions of the Creative Commons Attribution (CC BY) license (<http://creativecommons.org/licenses/by/4.0/>).